ELSEVIER

Ceramics International 29 (2003) 745–756

CERAMICS INTERNATIONAL

www.elsevier.com/locate/ceramint

Solvent debinding mechanism for alumina injection molded compacts with water-soluble binders

Wei-Wen Yang[a,*], Kai-Yuan Yang[a], Moo-Chin Wang[b], Min-Hsiung Hon[a]

[a]*Department of Materials Science and Engineering, National Cheng Kung University, Tainan, Taiwan, ROC*
[b]*Department of Mechanical Engineering, National Kaohsiung University of Applied Sciences, Kaohsiung, Taiwan, ROC*

Received 11 March 2002; received in revised form 4 April 2002; accepted 10 November 2002

Abstract

The solvent debinding process has been widely accepted in the ceramic injection molding (CIM) industry process due to its short debinding cycle. However, the organic solvents most adopted in solvent debinding now are flammable, carcinogenic and not environmentally acceptable. For eliminating the use of unsound solvents, water-soluble polyethylene glycol (PEG) is used in this study to modify the pattern of debinding in CIM. The purpose of the investigation was to examine the binder behavior during solvent debinding based on water extraction for a multi-component PEG binder system. Based on the in situ evaluation results of dimensional variations, mercury intrusion data and scanning electron microscope (SEM) observations, possible solvent debinding mechanism for alumina injection molded compacts with water-soluble binders is proposed.

Keywords: A. Injection molding; B. Porosity; D. Al_2O_3; Solvent debinding

1. Introduction

Ceramic injection molding is a competitive manufacturing technology for producing geometrically complex parts from a wide range of materials [1–4].The processes including mixing, molding, debinding and sintering are dependent upon the types of binder used.

Among the debinding methods, thermal debinding is widely used as the major mean to remove organics before sintering. However, the evaporation of degraded products can cause pressure buildup within the green body and create voids at its center, bloating and cracks at its surface if thermal debinding is carried out hastily [5–8].

In order to overcome these problems in thermal debinding, solvent debinding [9,10] has been widely adopted by the industry. In the solvent debinding process, a portion of the binder can be chemically removed by using solvents like acetone, trichloroethane or heptane. A large amount of open porosities, after solvent debinding, allows the degraded products to diffuse to the surface easily. Therefore the subsequent thermal removal of insoluble binder components can be finished as short as 3 or 4 h.

Although solvent extraction is probably the fastest debinding route, a problem with solvent debinding concerns the nature of common solvents; the organic solvents most adopted in solvent debinding now are flammable, carcinogenic and not environmentally acceptable. In addition, several types of defect could still occur during the solvent debinding step. These defects are mainly caused by the large dimensional changes when parts are immersed in the solvent, especially for organic solvents [11,12].

For eliminating the use of unsound solvents, application of water-soluble binder to ceramic injection molding is therefore developing. Rivers [13] and Fanelli et al. [14], used methyl, ethyl or hydroxypropyl/hydroxyethyl celluloses or cellulose-derived as agar, and agarose as water-soluble binders. The gelation characteristics of cellulose by controlling the gel temperature, gel strength, and the degree of water retention were applied to form the shapes during injection molding. Polyethylene glycol (PEG) was used by Hens et al. [15] and Cao et al. [16] as primary water-soluble binder to mix with acetal copolymers and polyvinyl buteral (PVB)

* Corresponding author.
E-mail address: cim@ms39.url.com.tw (W.-W. Yang).

0272-8842/02/$30.00
PII: S0272-8842(02)00226-2

or PMMA, OPEW etc. as binders for injection molding of stainless steel or nickel-iron alloy powders.

PEG is a polymer of ethylene oxide with molecular weight from 200 to 20,000 [17]. The unique characteristics of PEG is water soluble and thermoplastic. In addition, they are very safe chemicals and are used quite extensively in food industry.

Considerable efforts have been made to understand the transport of binder vapor and fluid in the molded compact during solvent debinding and thermal debinding [7,18–22]. None of these studies, however, has considered the debinding mechanism for CIM specimens during solvent debinding based on water extraction. The purpose of the investigation was to examine the binder behavior during solvent debinding based on water extraction for a multi-component PEG binder system. Mercury porosimetry and scanning electron microscopy (SEM) were employed to determine the pore structure and the binder distribution at different stages of debinding. In addition, the dimensional variations of alumina injection-molded compacts containing polyethylene glycol binder system during water extraction were also studied. From these results obtained, the debinding mechanism for CIM specimens during solvent debinding based on water extraction is proposed.

2. Experimental procedure

Commercial purity alumina powder (Japan, Showa Denko, AL-160-SG4) was used in the study to fabricate injection-molded specimens. The average particle size was 0.6 μm and specific surface area was 4.1 cm^2/g.

A multi-component binder system was used to prepare the alumina feedstock. For these binders, the major portion was PEG4000, the backbone consisted of polyethylene wax (PE wax) for good strength during debinding, and stearic acid (SA) was used for improving flow ability. The total alumina powder content was 55 vol.%, and the remaining 45 vol.% consisted of the aforementioned polymers with a weight ratio of PEG4000: PE wax: SA = 65:30:5.

Mixtures of alumina and binders were prepared by using a sigma-type blade kneader rotated at 50 r.p.m. The alumina powder was added first into the kneader and pre-heated at 100 °C for 30 min to achieve a homogeneous temperature distribution. The binders were then subsequently added to mix for 90 min. Granules were obtained by continuously rotating the blade during the cooling process to crush the mixture.

Viscosity of the feedstocks was measured in a Rosand capillary rheometer (RH-14), using the standard procedure

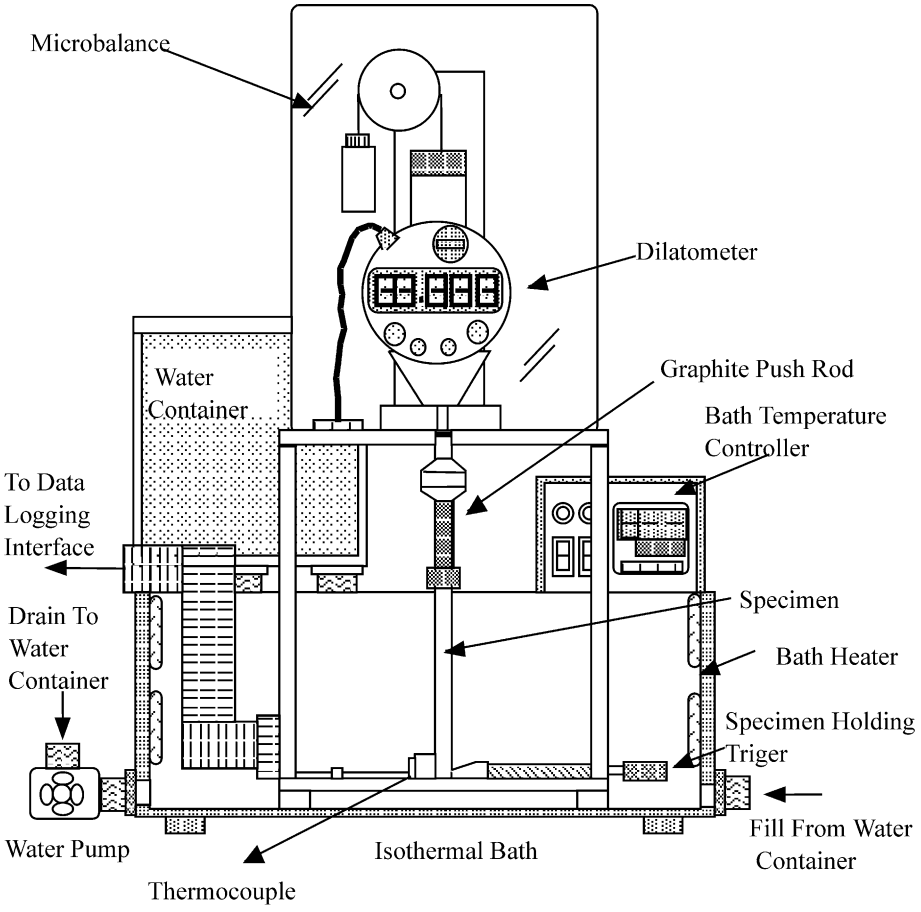

Fig. 1. The set-up of the dilatometer for measuring the length change of specimens during solvent debinding.

with temperature control of ±0.5 °C. Rectangular test bars with dimensions of 75×5×4 mm were injection molded at barrel temperature of 110 °C and die temperature of 40 °C. The test bars were then debound at 30–50 °C with water as solvent. For measuring the PEG extraction rate, the specimens were debound for different periods of time (5 min–8 h) and dried at 40 °C for 48 h.

A dilatometer was designed for monitoring the length changes of compacts in situ, as shown in Fig. 1. In this setup, a thermocouple was employed for recording the temperature variations of the specimen during solvent debinding. The alumina injection molded compact was fixed at one end and came into contact with the dilatometer directly at the other end. The weight of the graphite push rod, as indicated in Fig. 1, was offset by the microbalance. To simulate the case where the molded parts were immersed into a preheated water bath, water was preheated in a water container. Once the temperature of the water was stable, the preheated water was introduced into the isothermal sample tank. The length changes of the specimens were measured by the dilatometer as the solvent debinding proceeded.

To analyze the pore structure evolution during solvent debinding, a mercury porosimeter (Autopore II 9220, Micromeritics Instrument Co., USA) was used to measure the pore size distribution of samples taken at different solvent debinding stages. In addition, the fracture surface of specimens after being debound for different periods of time was observed by SEM (Jeol-5200, Jeol, Japan).

3. Results and discussion

3.1. Rheology and debinding rate

The effect of temperature and shear rate on the viscosity of feedstock used in this study is shown in Fig. 2. It apparently exhibited pseudoplastic flow behavior and the shear viscosity decrease with the shear rate for all the working temperature. The decrease in viscosity with increasing shear rate indicates particle (or binder molecule) orientation and ordering with flow, and may reflect improved homogeneity. In addition, it has been suggested that for ceramic injection molding, the shear rates can vary from 100 to 1000 s^{-1} and the flow rate during molding requires a viscosity less than 1000 Pa s [23,24]. Viscosities of feedstocks with PEG binders match the request.

In the study, water was used as the solvent for extracting soluble binder PEG from molded compacts. Fig. 3 shows the effect of debinding temperature on the extraction of PEG from 30 to 50 °C for various debinding times. A higher efficiency was achieved as

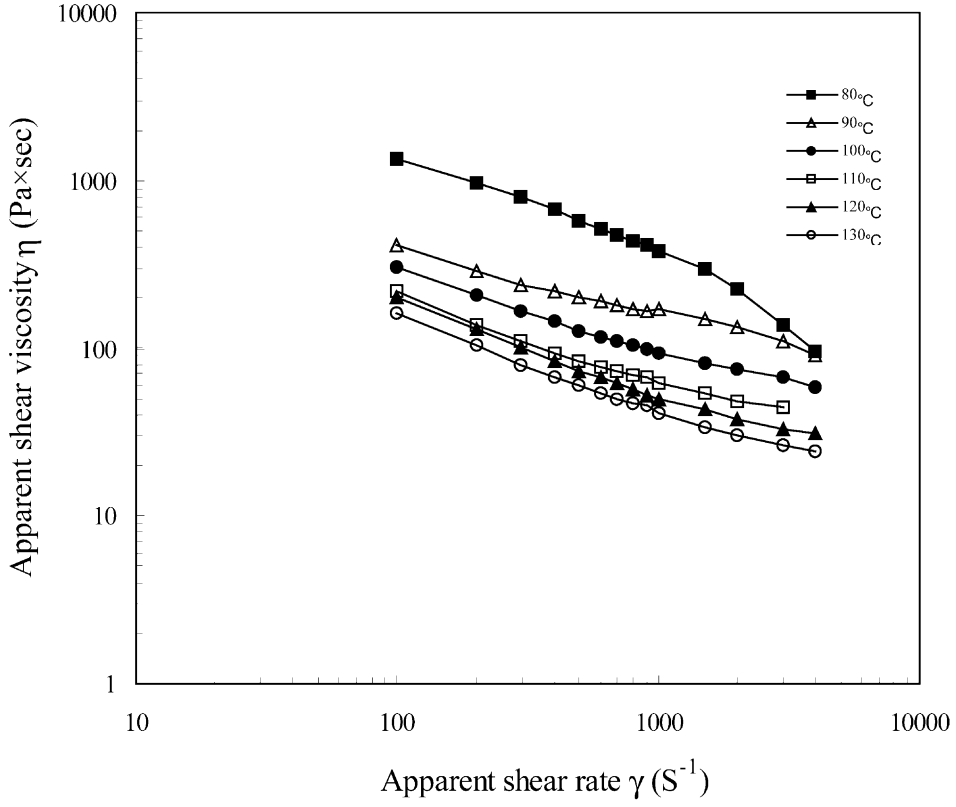

Fig. 2. Apparent shear viscosity versus apparent shear rate for feedstock with PEG binder system at different temperatures.

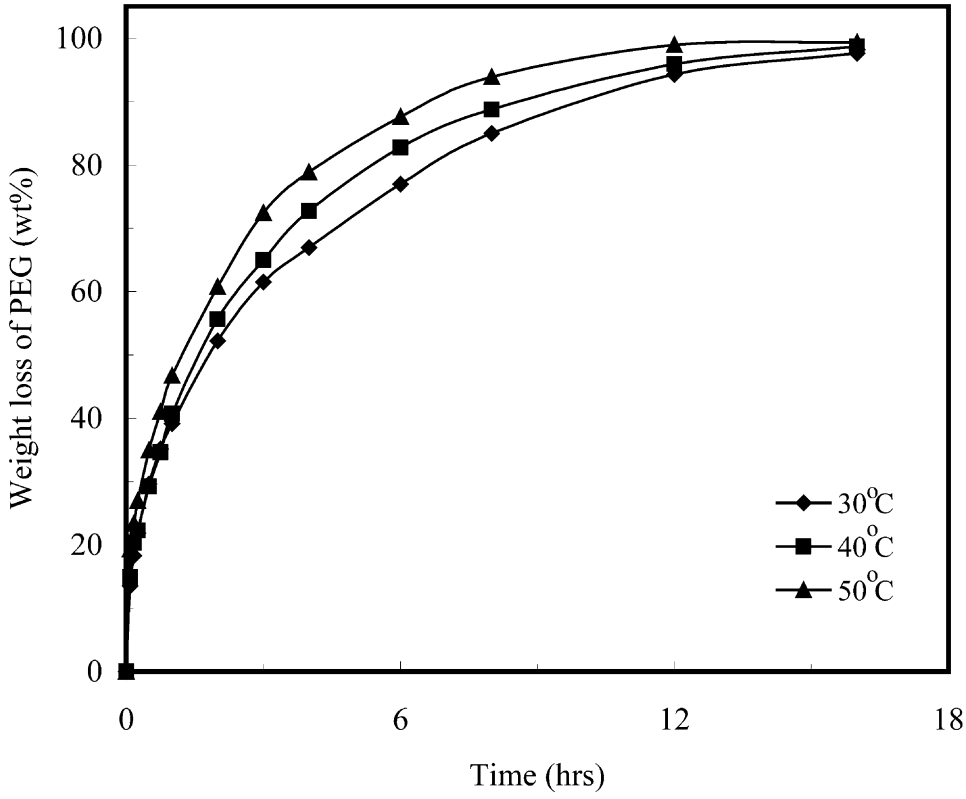

Fig. 3. Effect of debinding temperature on the weight loss of alumina compact immersed in water for various extractive times.

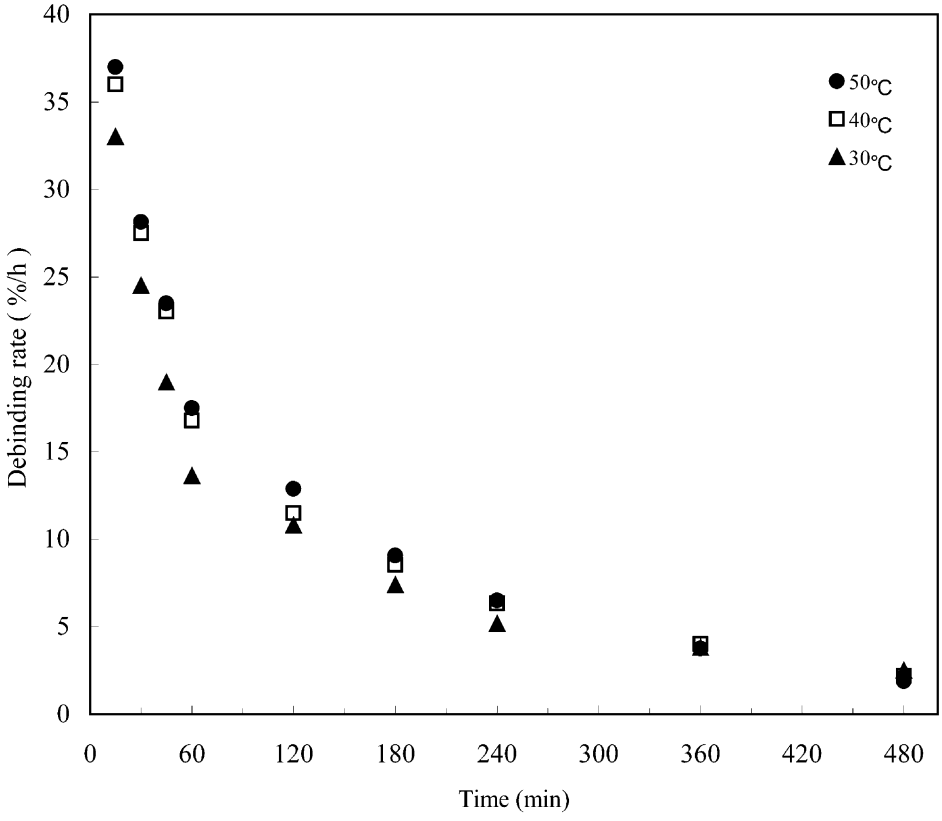

Fig. 4. Debinding rate as a function of the debinding time for alumina compacts immersed in water at 30–50 °C.

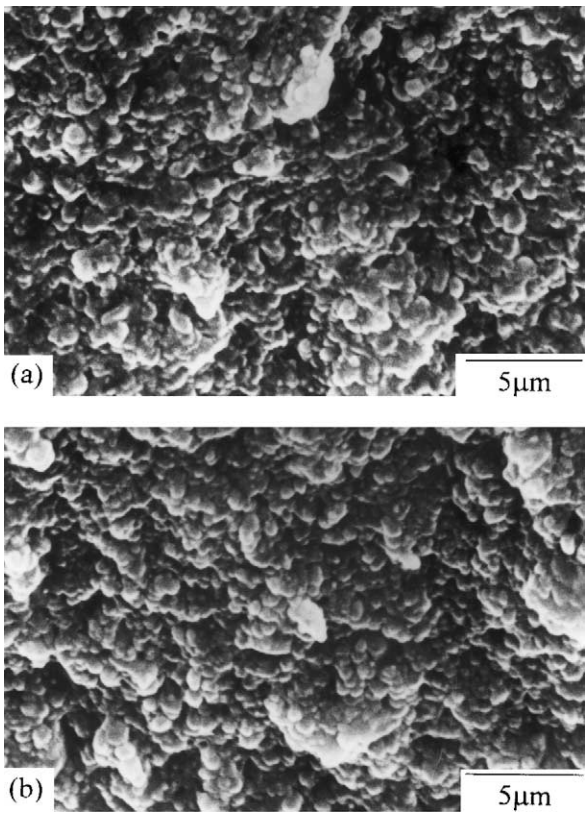

Fig. 5. SEM morphology of cross section near the (a) surface (b) center for samples as molded.

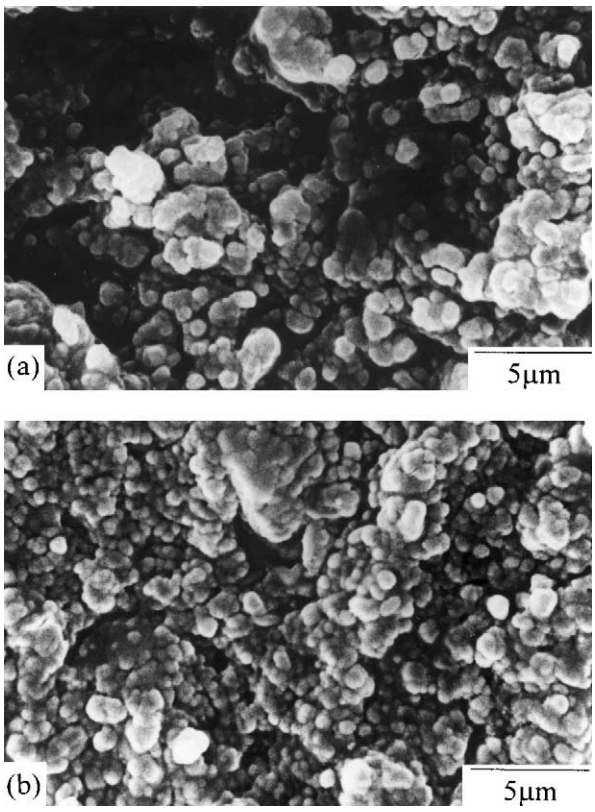

Fig. 7. SEM morphology of cross section near the (a) surface (b) center for samples debound in water at 40 °C for 2 h.

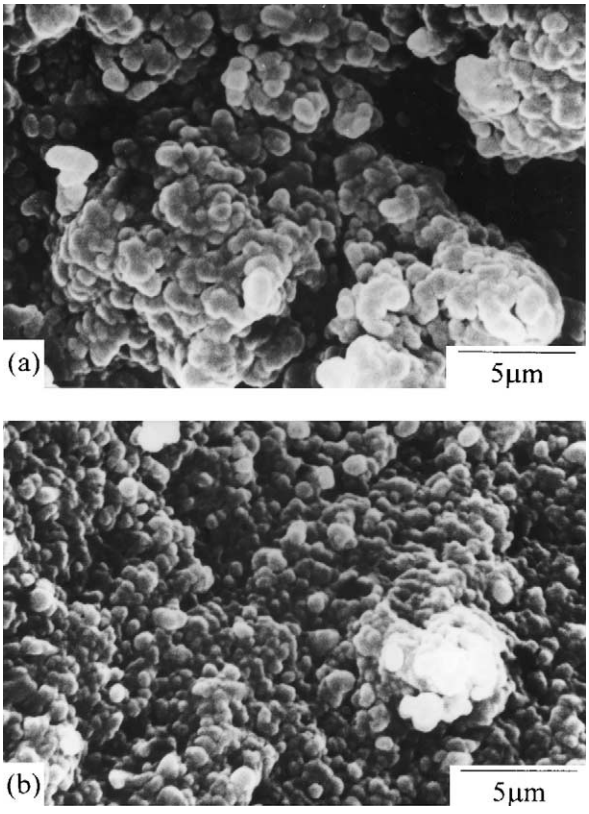

Fig. 6. SEM morphology of cross section near the (a) surface (b) center for samples debound in water at 40 °C for 5 min.

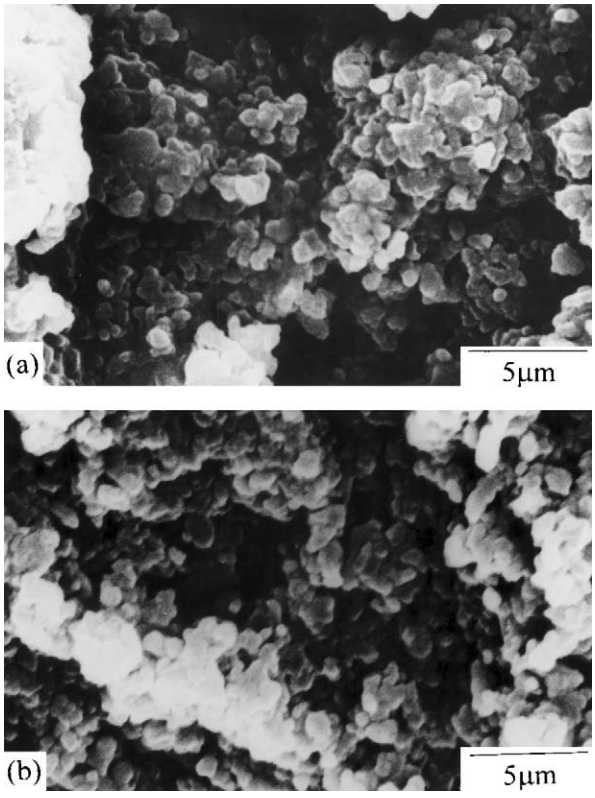

Fig. 8. SEM morphology of cross section near the (a) surface (b) center for samples debound in water at 40 °C for 3 h.

debinding temperature was increased due to a larger solubility and diffusivity of PEG in water at higher temperature. In addition, the debinding rate, determined from the slopes in Fig. 3, was decreased when the debinding time increased as showed in Fig. 4.

3.2. SEM observation

Figs. 5–8 show, respectively, the morphology of the outer edge and center of green part and samples debound in the water bath at 40 °C for different periods of time. For 5-min solvent-debound parts, the morphology at the outer edge, as shown in Fig. 6(a), demonstrates that pores with different sizes were formed. Some were interparticle pores and some were within the binders, indicating that the soluble binder (PEG) had been extracted. Similar examinations were also made for the center region of fractured specimens. Fig. 7(b) shows that there was still no pore generated in the center region of the specimen after being debound for 2 h, indicating that the PEG still did not dissolve at this time. Some pores were not observed in the center region until the end of 3 h debinding, as demonstrated in Fig. 8(b). The consequences indicate that the PEG dissolution started from the surface and progressed toward the center of the specimen, and 3–4 h were needed for water to penetrate into the center of the specimen and interact with the all PEG molecules at 40 °C.

3.3. Pore structure development in debinding

Fig. 9 shows cumulative pore volume vs. pore diameter for samples extracted from the solvent bath at different periods of time. For green parts, it is observed that some large pores existed at low mercury pressures. These cavities were formed due to the pullout of powders as tensile bars were fractured into smaller pieces. As the mercury pressure in testing was increased, a series of small pores were detected.

After debinding for 5 min, as the mercury pressure was increased, a sharp increase in pore volume was noted at the pore size of 0.3 μm. Following this, there is a plateau between 0.2 and 0.03 μm, which is the limit of the detectable pore diameter for the instrument used. The curve indicates that most pores were between 0.2 and 0.3 μm.

When the debinding time increased, the shapes of the mercury intrusion curves of the samples were similar to

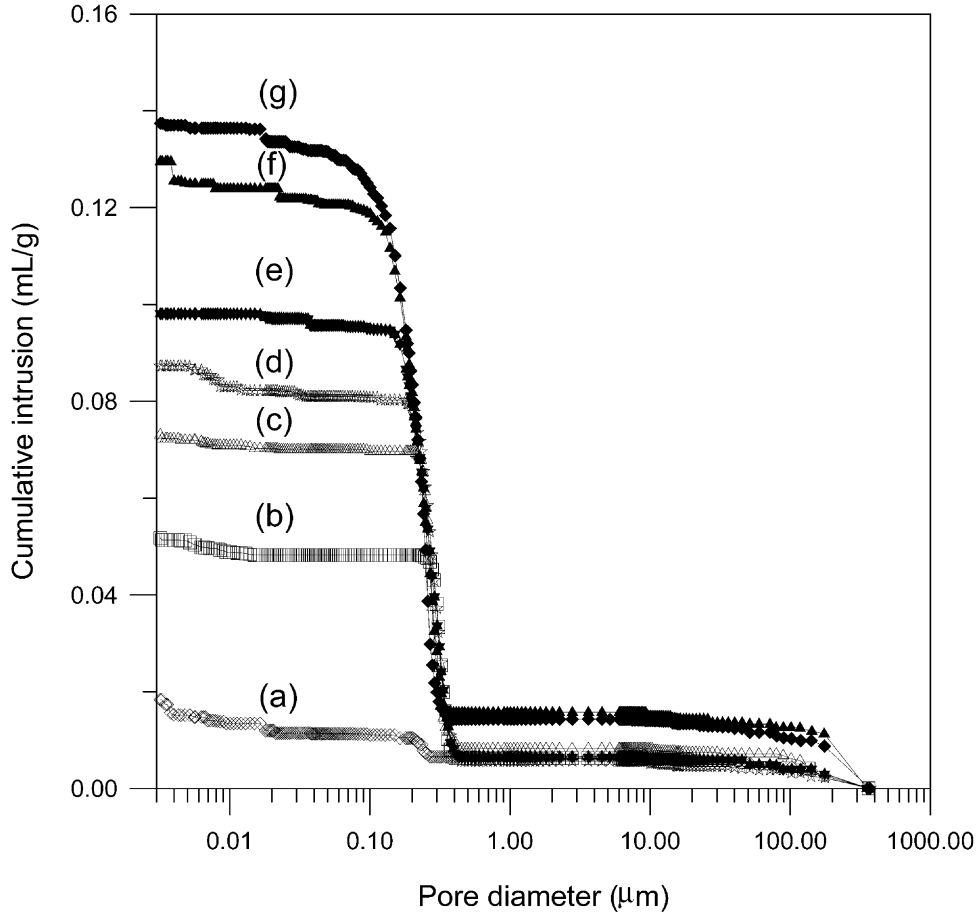

Fig. 9. Relationship of cumulative pore volume and pore diameter for (a) green part and specimen extracted in water for (b) 5 min, (c) 30 min, (d) 1 h, (e) 2 h, (f) 4 h, (g) 8 h.

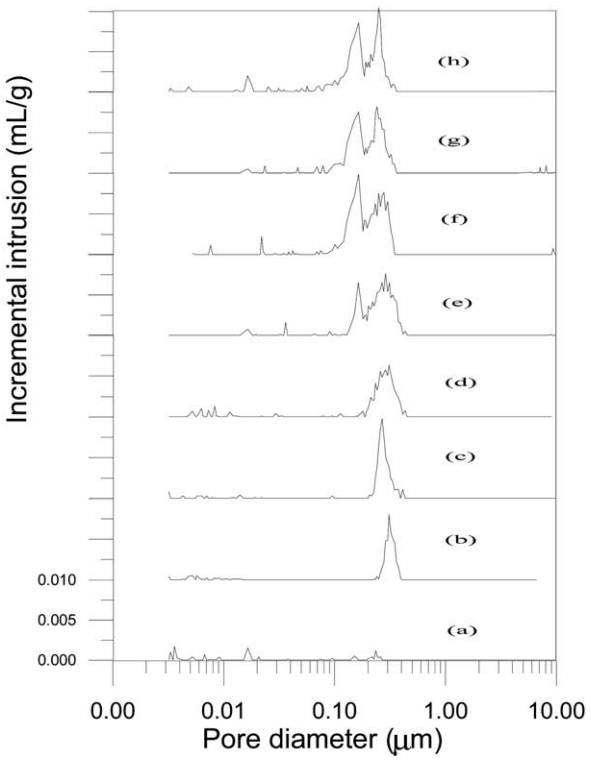

Fig. 10. Relationship of incremental pore volume and pore diameter for (a) green part and specimen extracted in water for (b) 5 min, (c) 30 min, (d) 1 h, (e) 2 h, (f) 4 h, (g) 6 h, (h) 8 h.

that for 5 min debinding. However, the cumulative volume of pores increased.

Relationship of incremental pore and pore diameter for specimens extracted in water for different periods of time is shown in Fig. 10. At the beginning of debinding, the PEG at the surface of specimen dissolved in water when alumina compacts were immersed in water, however, the water did not diffuse into the interior of specimen yet, so the distribution of pores was narrow and the pore size was almost near 0.3 μm. [Fig. 10(b)].

As the debinding time increased (30 mins–1 h), as the results of fine pores generated at the beginning, water molecules could diffuse into the interior of specimen gradually and some small pores could be observed, however, the distribution of pores did not broaden obviously.

As the debinding time continued to 2 and 3 h, the solvent-debound depth increased as observed by SEM, more water penetrated into the binder and thus more fine channels were formed. The pore size and pore volume increase and the distribution of pores broaden obviously. It showed that the interconnected pore channel was formed at this moment.

3.4. Dimension change

Fig. 11 shows the length and temperature changes of alumina specimens after being immersed in water at

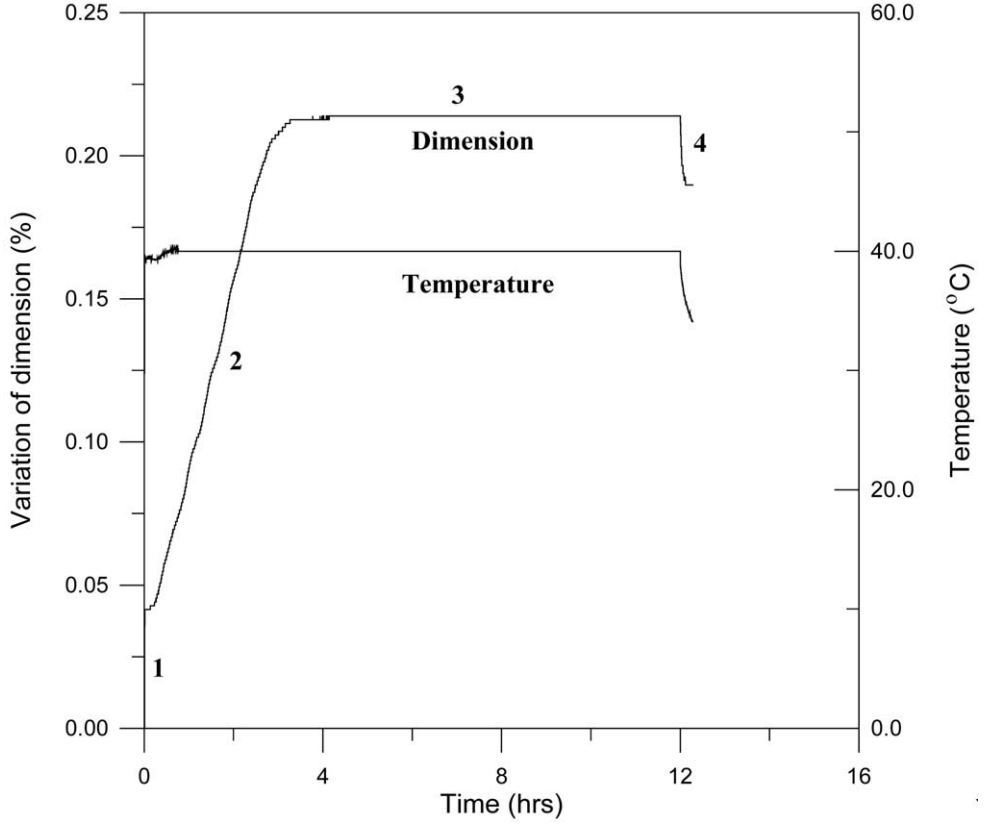

Fig. 11. The changes of length and temperature for alumina compacts immersed in water at 40 °C for different periods of time.

40 °C for different periods of time. The curve of dimension change could be divided into four stages. In the first stage, the parts expanded drastically as soon as they came into contact with the preheated water. After the initial sharp expansion, molded compacts expanded slowly and reached a total expansion of about 0.21% after 3.5 h debinding. The dimension of the specimen was unchanged in the third stage. Finally, the parts shrank drastically when water was drained out.

The sharp dimensional change occurred when the water was introduced into or drained from the sample tank corresponding with the temperature change, as shown in Fig. 11. The sharp increase and decrease at the beginning and the end of debinding respectively can be assumed to be as a result of thermal expansion.

In contrast to the thermal expansion in the first stage, the cause of mild expansion in the second stage could be related to the debinding. It has been postulated that dissolution of binder is a slow process that occurs in two stages [25]. First, solvent molecules slowly diffuse into the binder to produce a swollen gel. If the molecular interaction is large because of cross-linking, crystallinity, or strong hydrogen bonding, then swelling of the binder results. If the attraction between the polymer and solvent is larger than the interaction between polymers, then the second stage of binder dissolution can take place. Here the gel gradually disintegrates into a true solution.

The binder system used in the experiment was composed of PEG4000, PE wax and SA. The effect of SA was ignored because the quantity of SA was very small. Fig. 12 shows the length changes of the pure PE wax specimens after being immersed in water, ranging from room temperature to 40 °C. There was no swelling except thermal expansion, the expansion in the second stage therefore must have been due to the interaction between PEG and water.

In addition, the dimensional variation as indicated in Fig. 11, reached a stable value after being debound for 3.5 h. It matched the time needed for water to penetrate into the center of the specimen and interact with the PEG molecules as observed by SEM.

3.5. Debinding mechanism

According to the above results that water slowly diffused into the PEG to produce a swollen gel at the beginning when water was used as the solvent for extracting soluble binder PEG. If the attraction between the PEG and water molecules is larger than the interaction

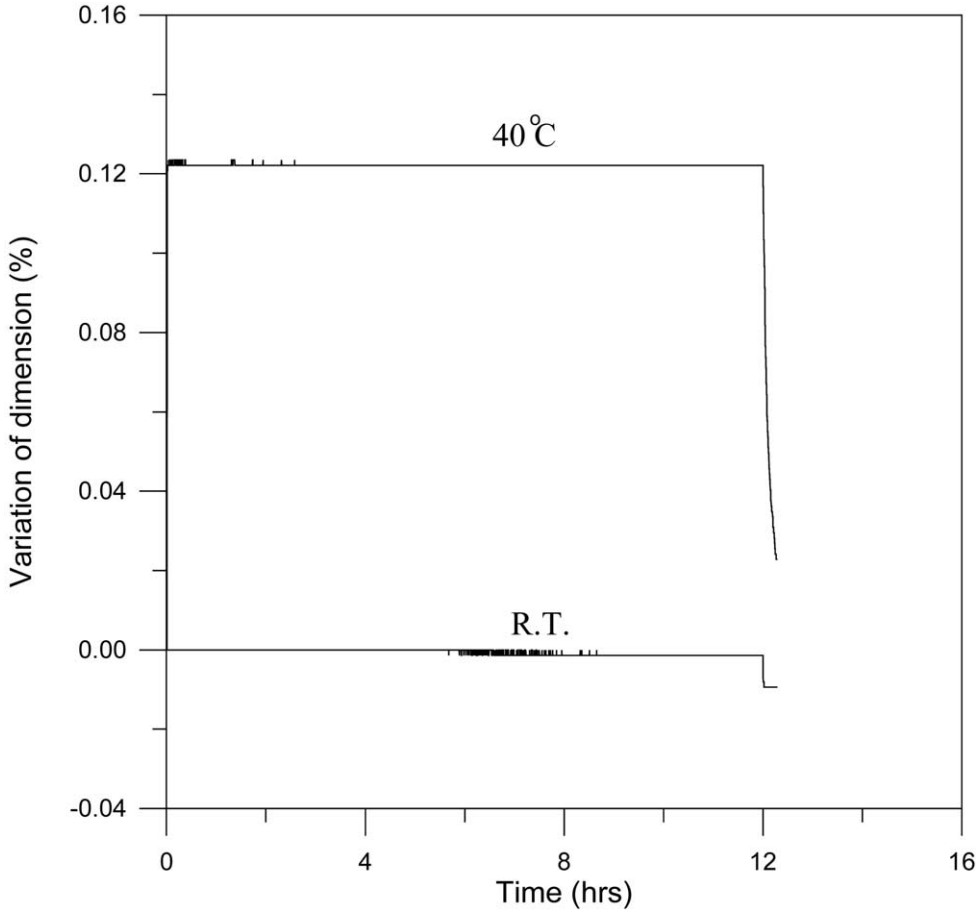

Fig. 12. The length changes of pure PE wax compacts immersed in water for different periods of time at different temperatures.

between polymers, the second stage of binder dissolution can take place. Here the gel gradually disintegrates into a true solution and the absorbed water content now could be defined as equilibrium water content (EWC) [26].

$$\mathrm{EWC} = \frac{\text{weight of swollen gel} - \text{weight of dry gel}}{\text{weight of swollen gel}}$$

The PEG starts dissolving when the water concentration in PEG gel is larger than the EWC of PEG.

Based on the in situ evaluation results of dimensional variations, mercury intrusion data and SEM observations as presented earlier, possible solvent debinding mechanism for alumina injection molded compacts with water-soluble binders is discussed as follows.

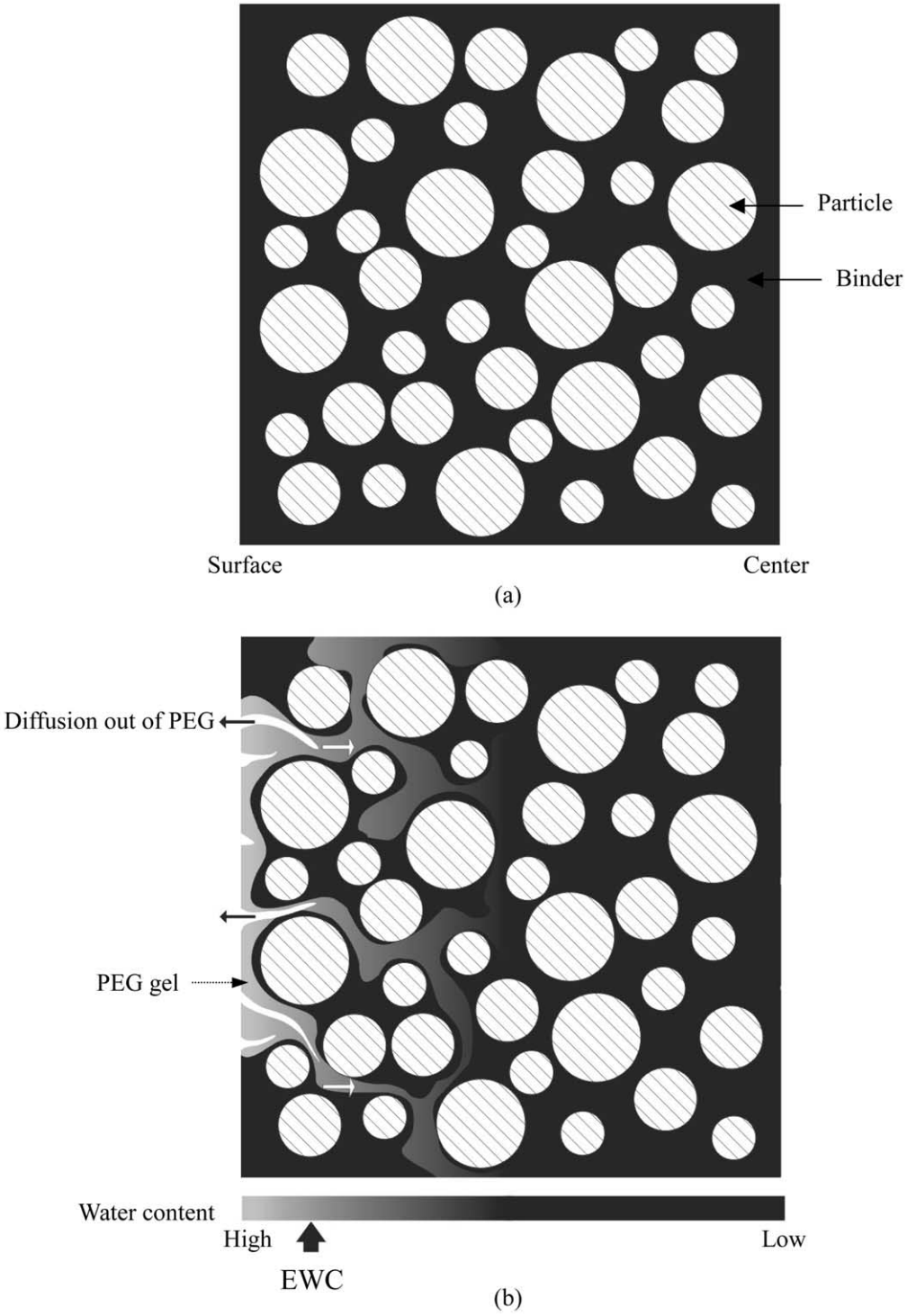

Fig. 13. The schematics of binder distributions at the (a) as-molded and (b) initial of solvent debinding based on water extraction.

3.5.1. Initial stage

As molded parts were immersed in the solvent bath, parts expanded drastically as soon as the parts came into contact with preheated water as a result of the temperature increase. After the initial sharp thermal expansion, water diffused into the PEG to produce a swollen gel and the swollen force expands the specimen. When the water content in PEG gel was larger than the EWC of PEG, the PEG started dissolving. The water content decreased with the depth of specimen because

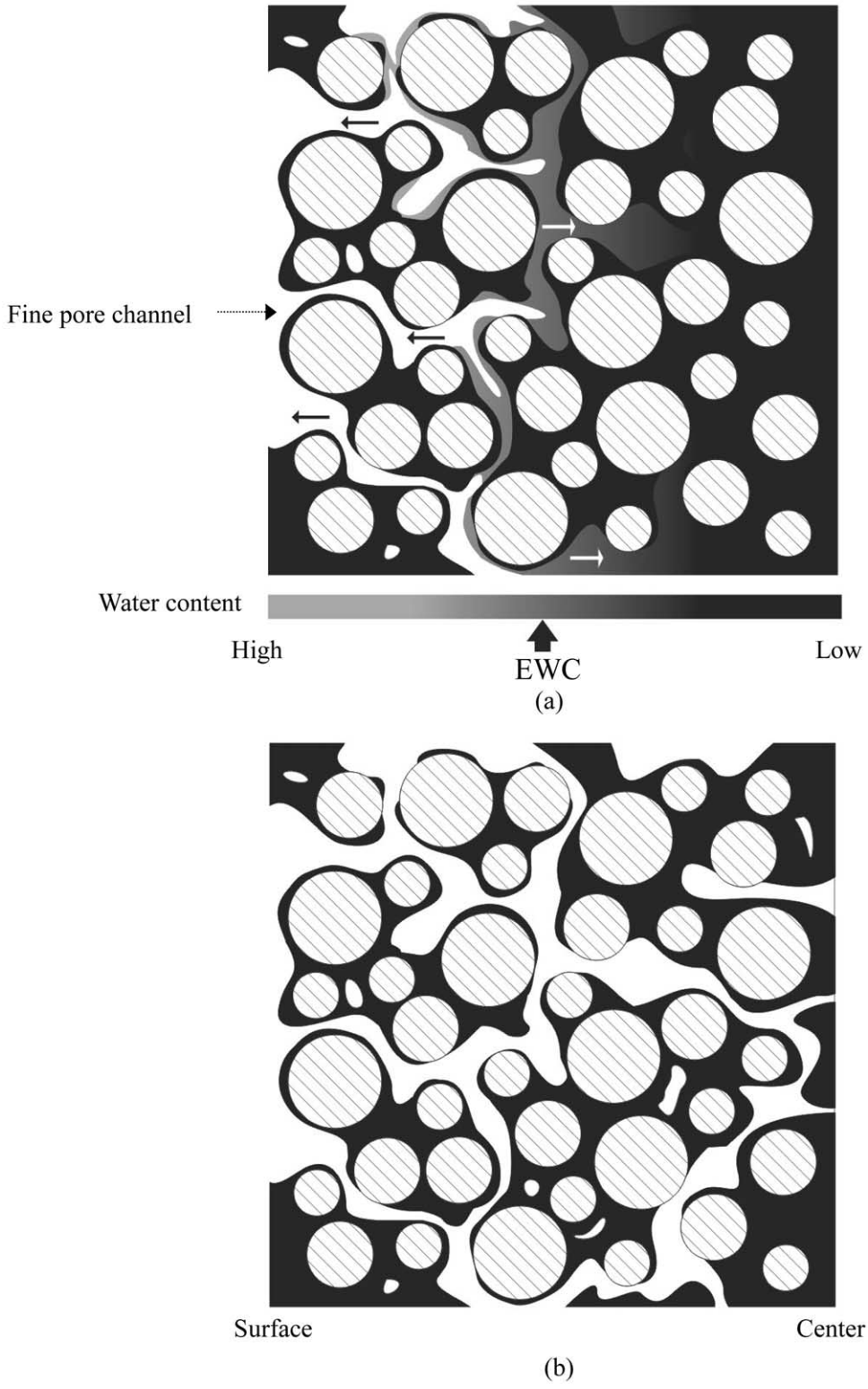

Fig. 14. The schematics of binder distributions at the (a) intermediate and (b) final stages of solvent debinding based on water extraction.

the water diffused into the specimen from the exterior to interior slowly through the pores. Only PEG at the surface began dissolving into the solvent at this stage, and fine pore channels were left behind [Fig. 6(a)]. The distribution of pores was narrow and the pore size are almost near 0.3 μm [Fig. 10(b)–(d)], as illustrated in Fig. 13(b).

3.5.2. Intermediate stage

As debinding continued, the PEG molecules would swell gradually to form gel from the exterior to interior of the specimen when the PEG molecules came into contact with water; consequently, the swell forced the specimen to expand continuously. In addition, the solvent-debound depth increased as observed by SEM. Fig. 14(a) shows the schematics of binder distributions at the intermediate stage of solvent debinding. Owing to the increase of water content in the interior of specimen, the depth where the water content exceed the EWC extended and the solvent-debound depth increased with the debinding time.

Furthermore, new pores continued to form as water penetrated into the interior of specimen gradually and provided more binder-solvent interfaces, which could increase the debinding rate. However, the debinding rate decreased with the debinding time as shown in Fig. 4. Since the inter-diffusion distance for the water and PEG is short in the initial stage, the debinding rate was quite fast. As debinding proceeded, the pore channels extended to the inner region of the parts, a longer diffusion distance slowed down the debinding rate.

3.5.3. Final stage

As the debinding time continued to 2 and 3 h, the pore size and pore volume increased and the distribution of pores broadened obviously. When water penetrated into the center of specimen (about 3.5 h) and the equilibrium between PEG and water was reached, the total dimensional variation reached the maximum value and the dimension remained constant (Fig. 11). Fig. 14(b) shows the schematics of binder distributions at the final stage of solvent debinding. It shows that the interconnected pore channels were formed from exterior to interior, leaving the insoluble binders in the contact region and the pore channels could serve as escape paths for decomposed gas during subsequent thermal debinding for insoluble binders.

4. Conclusions

During solvent debinding based on water extraction, the molded parts expanded drastically as soon as the parts came into contact with preheated water as a result of temperature increase. Then the PEG molecules would swell gradually to form gel from exterior to interior of the specimen when the PEG molecules came into contact with water, consequently, the swell forced the specimen to expand continuously. When the water content in PEG gel was larger than the EWC of PEG, the PEG started dissolving.

As debinding continued, owing to the increase of water content in the interior of specimen, the depth where the water concentration exceed the EWC extend and the solvent-debound depth increased with the debinding time.

As the debinding time continued to 2 and 3 h, the pore size and pore volume increased and the distribution of pores broadened obviously. When water penetrated into the center of specimen (about 3.5 h) and the equilibrium between PEG and water was reached, the total dimensional variation reached the maximum value and the dimension remains constant. It shows that the interconnected pore channels were formed from exterior to interior, leaving the insoluble binders in the contact region and the pore channels could serve as escape paths for decomposed gas during subsequent thermal debinding for insoluble binders.

Acknowledgements

The authors wish to thank the National Science Council of Taiwan, ROC for the support of this work under the project (NSC-87-2216-E-006-042).

References

[1] T. Chartier, E. Delhomme, J.F. Baumard, G. Veltl, F. Ducloux, Injection moulding of hollow silicon nitride parts using fusible alloy cores, Ceram. Int. 27 (7) (2001) 821–827.
[2] S.I.-En. Lin, Near-net-shape forming of zirconia optical sleeves by ceramics injection molding, Ceram. Int. 27 (2) (2001) 205–214.
[3] H.Y. Juang, M.H. Hon, The effect of calcinations temperature on the behaviour of HA powder for injection molding, Ceram. Int. 23 (5) (1997) 383–387.
[4] T. Zhang, J.R.G. Evans, J. Woodthorpe, Injection moulding of silicon carbide using an organic vehicle based on a preceramic polymer, J. Eur. Ceram. Soc. 15 (1995) 729–734.
[5] G. Bandyopadhyay, K.W. French, Injection molded ceramics: critical aspects of the binder removal process and component fabrication, J. Eur. Ceram. Soc. 11 (1993) 23–34.
[6] K.S. Hwang, T.H. Tsou, Thermal debinding of powder injection molded parts: observations and mechanisms, Metall. Trans. 23A (1992) 2775–2782.
[7] H. Verweij, W.H.M. Bruggink, Reaction-controlled binder burnout of ceramic multilayer capacitors, J. Am. Ceram. Soc. 73 (1990) 226–231.
[8] J. Woodthorpe, M.J. Edirisingheand, J.R.G. Evans, Properties of ceramic injection moulding formulations. Part 3: polymer removal, J. Mater. Sci. 24 (1989) 1038–1048.
[9] K.P. Johnson, US. Patent 4765950, 23 August 1988.
[10] R.E. Wiech, Jr., US Patent 4197118, 8 April 1983.
[11] R.M. German, Powder Injection Molding, Metal Powder Industries Federation, Princeton, NJ, USA, 1990.

[12] H.E. Amaya, Solvent dewaxing: principles & application, in: Proceedings of the Powder Metallurgy Conference Advances in Powder Metallurgy 3, 1990, pp. 233–246.
[13] D. Rivers, US Patent 4113480, 1978.
[14] A.J. Fanelli, R.D. Silvers, W.S. Frei, J.V. Burlew, G.B. Marsh, New aqueous injection molding process for ceramic powders, J. Am. Ceram. Soc. 72 (1989) 1833–1836.
[15] K.F. Hens, R.M. German, Advanced processing of advanced materials via powder injection molding, in: A. Lawley, A. Swanson (Eds.), Advances in Powder Metallurgy and Particulate Materials, Vol. 5, Metal Powder Industries Federation, Princeton, NJ, 1993, pp. 133–142.
[16] M.Y. Cao, J.W.O. Connor, C.I. Chung, A new water soluble solid polymer solution binder for powder injection molding, in: Powder Injection Molding Symposium, 1992, pp. 85–98.
[17] L.D. Berger Jr., M.T. Ivison, Ethylene oxide polymer, in: R.L.D. Davidson, M. Sittig (Eds.), Water-Soluble Resins, Chapman and Hall, London, 1963, pp. 169–201.
[18] H.M. Shaw, M.J. Edirisinghe, Porosity development during removal of organic vehicle from ceramic injection mouldings, J. Eur. Ceram. Soc. 13 (1994) 135–142.
[19] H.M. Shaw, M.J. Edirisinghe, Shrinkage and particle packing during removal of organic vehicle from ceramic injection mouldings, J. Eur. Ceram. Soc. 15 (1995) 109–116.
[20] B.K. Lograsso, R.M. German, Thermal debinding of injection moulded powder compacts, Powder Metall. Int. 22 (1990) 17–22.
[21] P. Calvert, M. Cima, Theoretical models for binder burnout, J. Am. Ceram. Soc. 73 (1990) 575–579.
[22] D.S. Tsai, W.W. Chen, Solvent debinding kinetics of alumina green bodies by powder injection moulding, Ceram. Int. 21 (1995) 257–264.
[23] M.J. Edirisinghe, J.R.G. Evans, Rheology of ceramic injection moulding formulations, Br. Ceram. Trans. J. 86 (1987) 18–22.
[24] M.J. Edirisinghe, J.R.G. Evans, Properties of ceramic injection moulding formulations, J. Mater. Sci. 22 (1987) 269–277.
[25] F.W. Billmeyer Jr., Textbook of Polymer Science, John Wiley & Sons, New York, 1984.
[26] A.B. Clayton, T.V. Chirila, P.D. Daltov, Hydrophilic sponges based on 2-hydroxyethyl methacrylate. III. Effect of incorporating a hydrophilic crosslinking agent on the equilibrium water content and pore structure, Polym. Int. 42 (1) (1997) 45–56.